Application of the Envelope Attribute to Seismic Data Visualization and Interpretation

[1]Uche Eberechi Ezebuiro*, [2]Levi Ikechukwu Nwankwo and [3]Clement Olufemi Akoshile
[1]Goodspac Online Nigeria Ltd., Lagos.
[2]Department of Physics, Federal University Kashere, Gombe, Nigeria.
[3]Department of Physics, University of Ilorin, Ilorin, Nigeria.

ABSTRACT

This research demonstrates the use of the envelope attribute to improve the visualization and interpretation of seismic data. Through this method, we can gain a clearer understanding of the structure of a reservoir and more accurately evaluate hydrocarbon reserves. The accuracy of reservoir estimates heavily relies on the precision of hydrocarbon contact maps. In the Petrel software, these maps are typically created utilizing well tops inserted at the hydrocarbon contacts. However, a significant limitation of this approach is that the resulting contact maps may not accurately align with any variations in the hydrocarbon contact in situations where the latter is not horizontal, unless the density of wells across the reservoir is sufficient. In our study, an envelope attribute cube was generated using the Petrel software and correlated the high-amplitude signatures in the gas reservoirs on the well section window. Subsequently, these signatures were filtered and extracted as seismic geobodies. These geobodies were used as direct hydrocarbon indicators and to create contact maps. The results showed that the envelope attribute can be used to identify gas migratory paths. They also indicated that geobody-based hydrocarbon contact maps are more accurate in delineating reservoir contacts unlike those obtained with scanty well tops data. In addition, the closures on the volume maps obtained with geobody-based hydrocarbon contacts aligned more accurately with the structural features in the field, providing a reliable means to derive more accurate reservoir volume estimates.

Keywords: Envelope Attributes, Visualization, Geobodies, Contact maps, Migratory paths

INTRODUCTION

The envelope attribute being one of the seismic attributes, has been used as direct hydrocarbon indicator in several research works on reservoir characterization. The use of the envelope attribute to identify soft sands containing hydrocarbons was first demonstrated in publications by Taner and Sheriff (1977) and Taner *et al.,* (1979), wherein they employed the Hilbert transform to calculate the amplitude, phase, and frequency of the seismic signal. The envelope attribute has only positive amplitudes and is proportional to the magnitude of the reflection coefficient. As such, it highlights main seismic features present in the data. It is a complex attribute calculated from the formula (Taner *et al.,* 1979):

$$E(t) = \sqrt{f(t)^2 + Hf(t)^2} \qquad (1)$$

In the equation above, the function E(t) is the seismic envelope, $f(t)^2$ is the complex signal and $Hf(t)^2$ is the Hilbert's transform of the complex signal. It is often referred to as the seismic envelope because it envelopes a seismic signal Other attributes derived from the same operation are the instantaneous phase and instantaneous frequency. It is a post-stack attribute and is obtained as a result of a mathematical operation on the seismic signal. Other attributes derived from the same operation are the instantaneous phase and instantaneous frequency. It is a post-stack attribute and its mathematical operation on the seismic signal is illustrated in Figure 1.

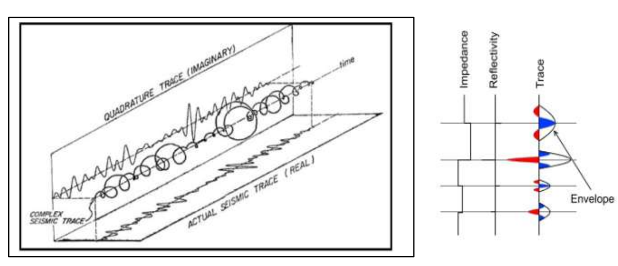

Figure 1: Components of the seismic attribute showing (a) the complex seismic trace (Taner *et al.* 1979) and (b) an illustration of the envelope trace (Yan *et al.* 2017).

Seismic attributes are essential in hydrocarbon

The authors wish to thank NNPC Limited, NNPC Upstream Investment Management Services (NUIMS), Goodspac Online Nigeria Ltd., Lagos. Department of Physics, Federal University Kashere, Gombe, Nigeria., Department of Physics, University of Ilorin, Ilorin, Nigeria and NAPE for providing the platform to present the paper during the Annual Conference.

exploration. Since the publications by Taner and Sheriff (1977) and Taner *et al.,* (1979), seismic envelope attributes have been widely used in hydrocarbon exploration. Nevertheless, the integration of envelope attributes in reservoir evaluation has gained wider acceptance and they are often used to complement conventional interpretations in any field of interest. For example, they are used as direct hydrocarbon indicators, particularly in areas without exploratory wells (Ismail and Zollo 2020), and to distinguish between hydrocarbon-bearing porous carbonate sections or boundaries (Sarhan, 2020). Additionally, seismic envelope attributes have been employed to study thin-bed tuning effects, unconformities, spatial correlation to porosity (Subrahmanyam and Rao, 2008), the prediction of fluid content (Nanda 2016), type of fluid contact (Oadfeul and Aliouane, 2014) and to map faults in different reservoirs (Ayolabi and Adigun 2013, Lacopini et al., 2016). Other applications in oil and gas exploration include predicting source rock distribution (Wang *et al.,* 2015) and identifying fluvial channels and their abundant depositional features (Alsouki *et al.,* 2014). These applications demonstrate the wide applicability of seismic attributes in the oil and gas industry.

Fluid contact refers to the boundary between fluids of different densities, and it plays a crucial role in hydrocarbon reservoirs. It's essential to comprehend the complexities of fluid contacts in these reservoirs because they are not always clearly defined or horizontally oriented as commonly depicted in models or diagrams. This is particularly true where there are transition zones and mixed phases in the reservoir, or where there is non-linear relationship between reservoir fluids (Dolson, 2016). In addition, the influence of semipermeable zones, hydrodynamic gradients, sandstone horizontality, and fault compartmentalization, can lead to variations in the depth and orientation of fluid contacts. This phenomenon is frequently observed in oil-wet reservoirs (Dolson, 2016). Other factors that contribute to irregularities in the depths of tilted oil-water contacts include reservoir heterogeneity, stemming from facies variations, bed thickness variations, faulting, and diagenetic permeability changes, (Dennis *et al.,* 2005). Consequently, accurately determining these contact depths across the reservoir is a challenging task. Relying on a single value for these depths can significantly impact estimates of fluid volumes and the development strategies for the reservoir. The illustrations in Figure 2 provide visual representations of scenarios that can result in tilted fluid contacts within hydrocarbon reservoirs:

One commonly used method of building reservoir contact surfaces involves inserting horizon tops at the gas-oil or oil-water contact depths during well log correlation. However, the accuracy of this method can be compromised if the well density is insufficient. This occurs because there may not be enough point data from the inserted horizon tops to construct accurate contact maps. Additionally, if the well trajectories do not intersect the contact points, the hydrocarbon contacts may not be visible on the well log correlation panels. Furthermore, even when contact types and depths are determined, this method may not accurately reflect the inclinations of the hydrocarbon contacts, particularly in dipping reservoirs. This study demonstrates the use of seismic geobodies extracted from the envelope attribute to create more accurate hydrocarbon contact maps for reservoir volume estimation, addressing the limitations of the traditional approaches.

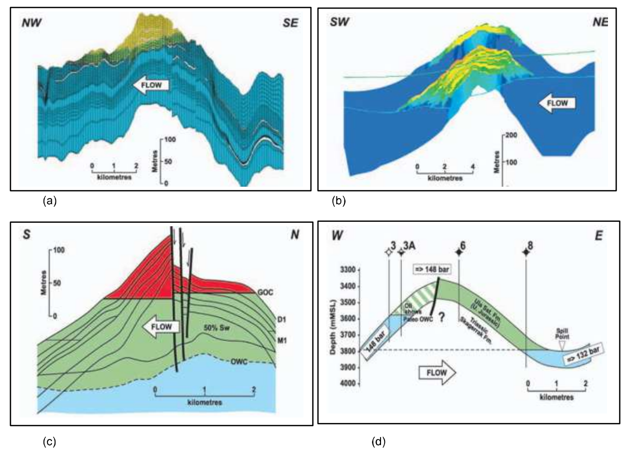

Figure 2: The presence of tilted hydrocarbon contacts, as exemplified in various case studies, can be attributed to the following factors: (a) A high-permeability reservoir overlying a low-permeability aquifer, as demonstrated in the 3D simulation of the Blane Field. b) Variations in permeability due to reservoir heterogeneity results in undulating original water contact (OWC) as it traverses different layers in the Ekofisk and Tor formations. (c) A low-permeability fault as seen in the DanField (Megson, 1992). The oil is interconnected across the fault, and the distinct OWCs are solely sustained by aquifer flow. (d) A hydrodynamic gradient induced by aquifer mobility, resulting in an OWC in the direction of lower aquifer pressure (Modified from Dennis *et al.,* 2005)

GEOLOGY OF STUDY AREA

The field under consideration will be referred to as 'Prima' field due to the proprietary rights of the dataset. It lies in the Niger-Delta depobelt which is considered one of the world's largest tertiary delta systems with substantial volumes of oil and gas (Turtle *et al,* 1999). It is located on the West African continental margin between which is the draining point for the Niger, Benue and Cross Rivers (Fig. 3). The Tertiary Niger-Delta consists of three formations that are distinguished based on sand-shale ratios. They include: the Akata Formation at the base of the delta which is composed of mainly thick shales, turbidite sand, and insignificant amounts of clay and silt and is about 7000 meter thick (Doust and Omatsola, 1990); the Agbada Formation which comprises paralic siliciclastics and is over 3700 meters thick (Turtle et al, 1999), and; the Benin Formation, which is made up of alluvial and upper coastal plain sands that are up to 2000 m thick (Avbovbo, 1978). Several researchers arrived at varying conclusions regarding the source of hydrocarbons in the Niger-Delta region.

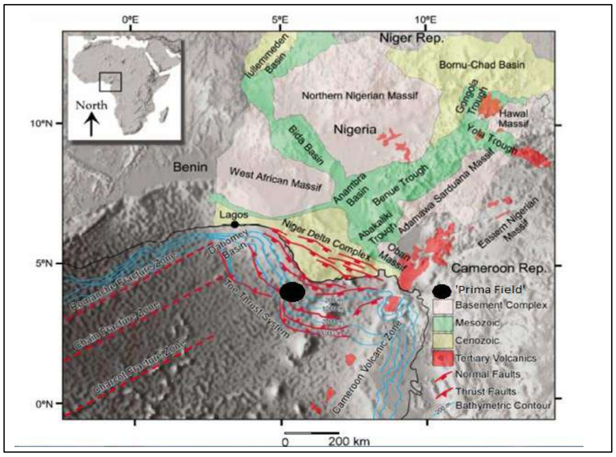

Figure 3: The location of the 'Prima' Field (encircled zone) within the Niger-Delta basin (modified from Corredor *et al.,* 2005).

Evamy *et al.,* (1978) proposed that both the Akata Formation and the lower Agbada Formation were the source rocks for the Niger Delta hydrocarbons. Ejedawe et al., (1984) concluded that in the central part of the delta, the Agbada shale is the source of the oil while the gas comes from the Akata Formation, indicating that both the Agbada and Akata Formations likely have distributed volumes of source rocks, the bulk of which is in the Agbada Formation. While Stacher (1995) proposed that the Akata shale is the only formation whose volume and depth of burial is in conformity with the characteristics of source rocks.

Corredor *et al.* (2005) conducted a characterization of the Niger Delta, identifying five distinct zones, each exhibiting unique structural styles. These zones include; passive, active, and reactive diapirs, shale overhangs and ridges, massifs and inter-diapir depocenters, which are indicative of the continental slope; an outer fold and thrust belt system with hinterland- verging and basinward thrust faults, along with associated folds; an extensive region situated beneath the continental shelf is typified by counter-regional growth faults, normal fault rollovers, and depocenters; a transitional detachment fold zone delineated by areas with minimal deformations and interspersed with detached folds positioned above the Akata formation; basinward thrust faults, inner folds, and associated detachment folds (Fig. 4).

Most reservoirs in the Niger-Delta basin were formed by structural traps during synsedimentary deformation of the

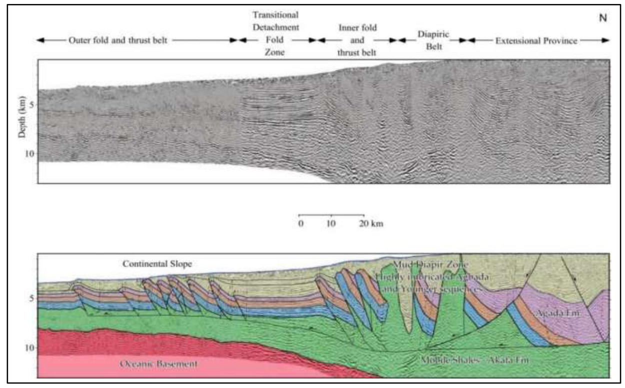

Figure 4: Structural interpretation of the regional seismic profiles across the Niger-delta (Corredor *et al.* 2005).

Agbada paralic sequence (Stacher, 1995; Evamy *et al.,* 1978). The trapping styles include simple rollover structures, antithetic faults, multiple growth faults, and collapsed crest structures (Doust and Omatsola, 1990; Fig. 5). The interbedded shales in the Agbada Formation constitute the main seal rock in the Niger-Delta. They provide seals by means of clay smears, vertical seals, juxtaposed lithological units and clay-filled canyons (Doust and Omatsola, 1990). Details of the Niger-Delta geology have been published in vaious research works including Weber and Daokoru (1975), Whiteman (1982) and Short and Stauble (1967).

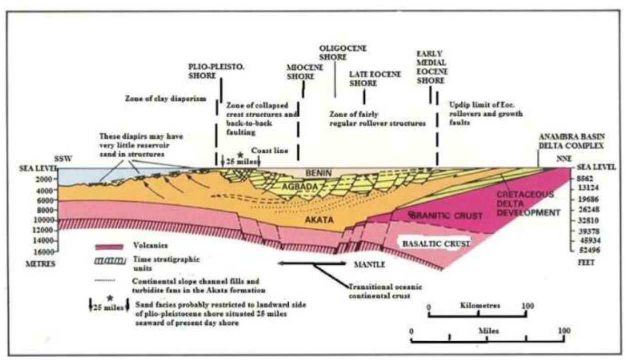

Figure 5: A cross-section of the Niger-delta showing the three stratigraphic units- the Benin, Agbda and Akata formations and their structural provinces (Whiteman, 1982).

METHODOLOGY

The correlation of well logs from the 13 wells revealed the presence of six distinct sands. To facilitate correlation, the wells were meticulously arranged based on their relative positions on the base map, starting with Well-A1 and concluding with Wells C3 and C11. Further analysis focused on the first and second sand due to their reservoirs containing both light oil and gas, which offer significant lithological contrast with the envelope attribute. The faults and interpreted seismic horizons corresponding to the cap rock and base rock of each sand unit, identified using seismic-to-well tie, were pivotal in generating the time and depth structural maps, forming the basis for each structural model. Average values of petrophysical properties such as net-to-gross, porosity, and water saturation were derived from empirical relationships and then upscaled into the 3D structural models to construct 3D petrophysical models. Complementing the interpretation, the envelope attribute cube was generated from the original amplitude volume. Notably, this cube was instrumental in highlighting gas accumulations with a distinctive yellow signature in the seismic volume.

In sandstone reservoirs, the existence of a gas cap results in a significant contrast in impedance, leading to a pronounced spike in the seismic signal's amplitude, particularly amplified by the envelope attribute. These high-amplitude zones, denoted by conspicuous yellow signatures, were further validated as hydrocarbon reservoirs based on the result of the correlation on the well section window and production data. These yellow signatures were used to examine the structure of the reservoirs and to better understand the interactions between them, providing valuable insight into the observations made during the well-log correlation and aiding seismic data interpretation.

The relationship between a gas cap or light oil and the envelope attribute also was meticulously employed in the extraction of seismic geobodies with the aid of the opacity filter and geobody extraction tools available in the Petrel software. Initially, the opacity filter was set to highlight the gas contents of the reservoir and these were extracted as seismic geobodies. From these, horizon interpretations were obtained from the undersurface of the extracted geobodies and with these, a contact map with the same size as the reservoir was built. The degree of alignment of the maps with the gas contact depths were viewed on the seismic section window and well correlation panels and cross-referenced with supplementary well gas contact data to ensure precision, given the potential alteration of depth range during map smoothening. Subsequently, the reservoir-sized gas contact maps were expanded beyond the reservoir boundary utilizing the convergent interpolation algorithm in the 'make surface' module of the Petrel software. This was done to determine whether the procedure could be used to obtain accurate contact surfaces for volume estimation. Also, utilizing the conventional approach the inserted horizon tops along the points of contact were used to build gas contact maps of similar size. Thereafter, the opacity filter of the inserted horizon was adjusted and extensive seismic interpretations from the geobodies were highlighted, extracted and used to build oil-water contact maps for all the reservoirs in Sands 1and 2. These contact maps were then duplicated, and their depth values bulk-shifted upwards to align with the previously identified gas contact depth. Finaly, the inserted horizon tops were utilized to build extensive oil contact maps of comparable size using the conventional procedure. These maps were meticulously compared on well-log correlation panels and the seismic section window, likewise the values of estimated oil and gas volumes and maps.

DISCUSSION OF RESULTS

The base map indicated three reservoir positions labeled as zones A, B, and C (Fig. 6). Zone A, located in the western part of the field, contains the first set of reservoirs and is serviced by a single well (Well-A1). Zone B, situated in the central part of the field, is home to eight drilled wells, while zone C is the location of Wells C-3 and C-11. Structural interpretations indicate that the reservoirs are fault-assisted, enclosed by the major fault, F1 (Fig. 6), and are vertically stacked (Fig. 7). The seismic-to-well tie has revealed horizons corresponding to the reservoir cap rocks on the seismic section window. The vertical profiles of the reservoirs, examined through the cross sections PP' and RR', demonstrate the effectiveness of the envelope attribute in identifying gas reservoirs and provide a window to visualize the comparison of the contact maps. Further justification for utilizing the envelope attribute for this study can be found in the high correlation between the gaseous hydrocarbons and the envelop attribute, as seen in the precise juxtaposition of the reservoir R2(B) and the golden signatures of the envelope attribute on the well log correlation window.

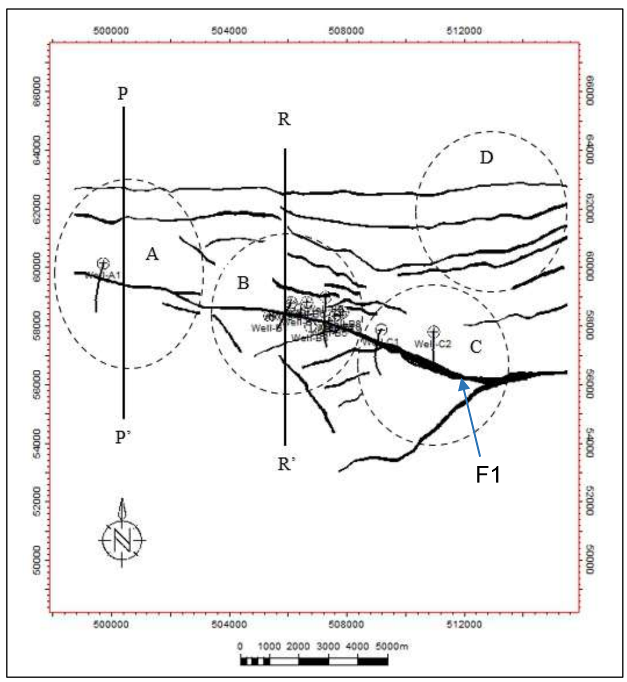

Figure 6: The base map of the 'Prima' field showing the positions of the wells, portions of the field where hydrocarbons are found (A, B, C, D) and the cross-sections that were considered in the study.

Application of the envelope Attribute to Structural Interpretation

The reservoirs in the first four sands were fault-assisted (enclosed by the major fault, F1) and were stacked vertically, while the reservoirs in the 5th and 6th sands were formed by a combination of structural and stratigraphic traps. The results from Sands 1 and 2 are significantly different because they contain oil and gas. A close examination revealed different links between the most of the reservoirs. For example, the envelope attribute identified a point of contact between reservoirs R1(B) and R2(B), indicating that the presence of gas in reservoirs R1(B), situated at the center of the field, had migrated from the gas cap of R2(B) through paths of structural weakness (Fig. 7a). Similarly, Figure 7b indicated that there exists a migratory path for hydrocarbons from Sand 5 through Sands 4, 3 and 2.

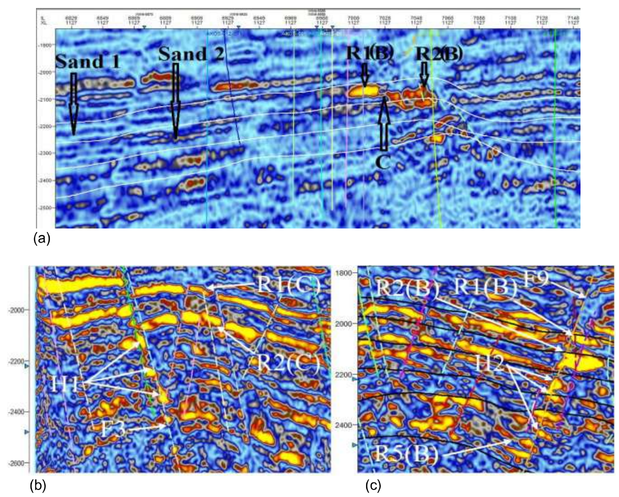

Figure 7: A screenshot of the seismic cross-section showing, in addition to the growth faults, (a) the link P, between reservoirs R1(B) in Sand 1 and reservoir R2(B) in Sand 2; (b) the migratory path (H1) of hydrocarbons from Sand 5 upwards along faults F3 and; (c) and the migratory path along fault F9 (H2).

The evidence for this conclusion came from production data for Well-B1, which confirmed the presence of a gas-oil contact in R2(B). Geobodies extracted from the area also showed the presence of gaseous hydrocarbons in the crevices of the cap rock of reservoir R5(B). These appeared as elongated columns of gas along the major fault line F1. The presence of these volumes of hydrocarbons along the fault lines indicates that some of the faults are not sealed.

Envelope Attribute as a Direct Hydrocarbon Indicator

The vertical profiles of the reservoirs examined through the cross sections PP' and RR' demonstrated the effectiveness of the envelope attribute in identifying gas and light oil reservoirs (Fig. 8). Seismic geobodies highlighted for the reservoirs in Sand 1 suggested the presence of small pockets of gas in zones B and C of the sand. However, the gas reservoirs and their associated contact maps were not visible on the well log correlation panels since the majority of the wells did not penetrate them due to their relatively small sizes (Fig. 8b).

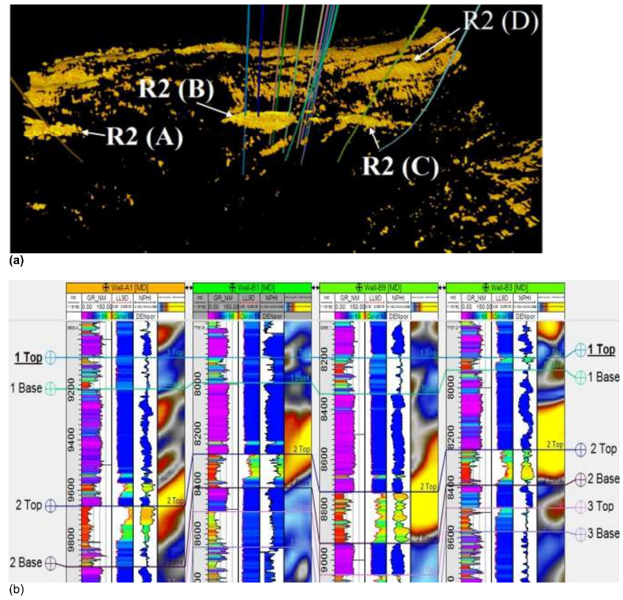

Figure 8: The workflow used in creating the hydrocarbon contacts: (a) the gas in zone B of reservoir 2 is identified on the seismic time slice of the envelope attribute cube, (b) the presence of the gas reservoir is correlated with the sand on the well section window. Sand 1 has comparatively smaller hydrocarbon volume captured on the well section window.

Other locations in Sand 2 highlighted by the envelope attribute as gas reservoirs were regions A and C and another in the northeastern part of the field (R2(D), (Fig. 8b)). A closer look at the correlation panels of Well-B3 (Fig. 8b) reveals the absence of the characteristic golden-yellow geobodies in Sand 3, which points to the absence of gas in the reservoir.

Application of the Envelope attribute in Hydrocarbon Contact Identification

The seismic geobodies representing gas accumulation within the reservoir units are depicted in Figure 9a. The corresponding three-dimensional bottom surface maps, derived from the interpretations of the extracted geobodies and accompanied by well locations, are presented in Figure 9b. It is important to note that the surface areas of these maps are confined to the peripheries of the extracted geobodies, consequently restricted to the reservoir boundaries. This limitation hinders their applicability in the volume estimation process. Nonetheless, the utilization of the envelope attribute in

R2(A) and R2(B) facilitated the differentiation of contact types in both reservoirs. These maps also enabled the correlation of hydrocarbon contacts observed in Well-A1 within the first reservoir, as well as those in Well-B9 and Well-B1 (R2B), albeit with challenges in distinguishing the latter contacts due to the shalier nature of the reservoir in comparison to Well-A1 (Fig. 10).

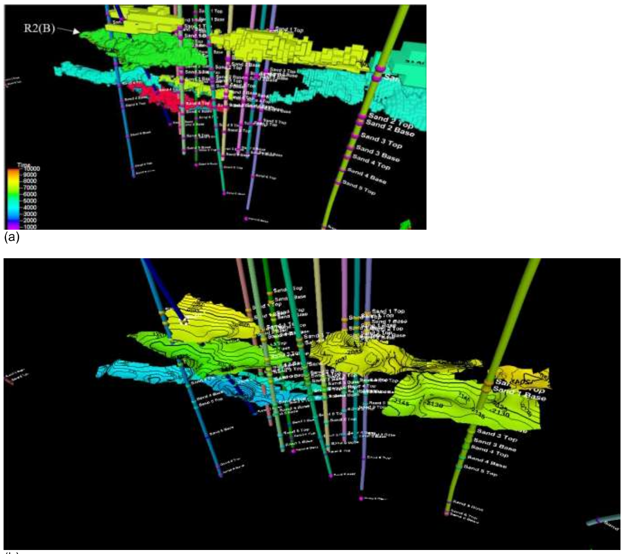

(a)

(b)

Figure 9: A 3D window showing: (a) the extracted geobodies and (b) the undersurface maps associated with each geobody used in identifying the gas contacts on the well-log correlation panels.

The primary advantage of this methodology lies in its ability to display individual contact maps on the well section window. The maps presented in Figure 10 have been aligned with the established contact in Well-B1, as documented in the production data. The utilization of the envelope attribute for correlating hydrocarbon contacts has effectively addressed the challenges posed by shale intercalations when determining gas-oil contact depths. In Well-B9, the presence of shale intercalations within the reservoir obscured the gas contacts in nearby wells, complicating their identification for correlation and subsequent contact map generation (Fig. 10). Notably, comparisons of the seismic time slice from the envelope attribute cube for reservoir R2(B) and the additional well data employed to establish hydrocarbon contact demonstrated strong correlations, aligning with fluid contact data for Well-B1 and other well logs on the well-section window. These steps effectively illustrate the multi-pronged approach used to determine the nature of contact within a reservoir and establish a robust foundation for employing this workflow to obtain hydrocarbon contact maps. Furthermore, the body-based contact maps exhibit enhanced accuracy by closely conforming to the dip of the gas contacts when viewed on the seismic section window (Figs. 10b and 10c).

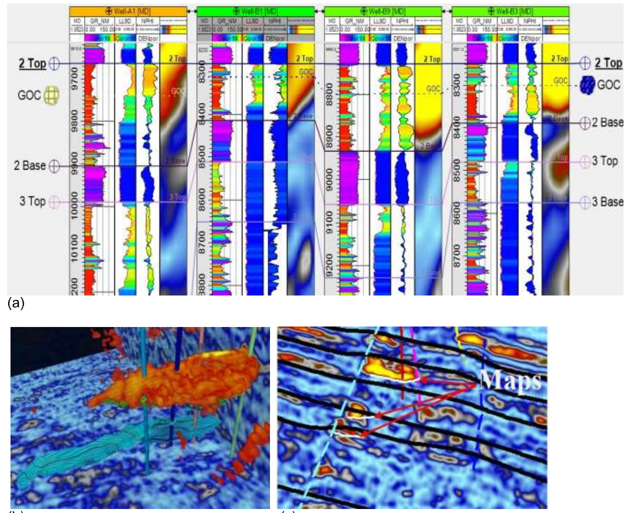

(a)

(b) (c)

Figure 10: The accuracy of the use of geobody-based contact maps is seen in accurate alignment of the contact maps on (a) the well section window, (b) on the seismic 3-D window and (c) RR' cross-section.

One major drawback though, is that the surface areas of those maps are insufficient for the hydrocarbon volume estimation module since their boundaries are limited to the edges of the reservoir. However, extrapolation of those maps to the boundaries of a closed polygon to enlarge them resulted in distortion in geobody-based map (Figs. 11a and 11b). This error is encircled in pink in Figure 11b and appears as the warped sides of the contact map in Figure 11c, while the obtained from inserted horizon tops was more stable along the horizontal plane (Fig. 11d).

The aforementioned maps were excluded from the volumetric calculation. However, the geobody-based contact maps exhibit a higher degree of adaptability by closely adhering to the inclination and topography of the hydrocarbon contacts within the reservoir than those obtained with inserted horizon tops. This disparity is indicated in the angle of inclination between the geobody-based maps and the former, denoted as 'h' in Figure 11b. A more comprehensive understanding can be garnered by examining how these fluids are retained within their respective reservoirs. According to general fluid dynamics, the positioning of hydrocarbons trapped at depth is anticipated to adhere to a density-dependent distribution, with the hydrocarbon contacts being perpendicular to the horizontal plane, as depicted in numerous illustrations. While this is typically the preferred scenario, deviations occur due to various factors expounded upon in prior sections. Consequently, unless adequately adjusted for, such hydrocarbon contact maps may yield inaccurate volume estimations.

The broader contact map provided increased flexibility, being derived from comprehensive seismic interpretations of the entire Sand 2 geobodies (Fig. 12). As

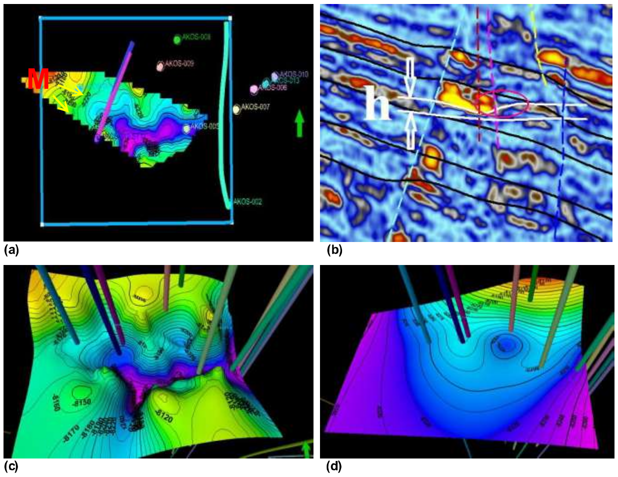

Figure 11: Comparison of the first contact maps built with geobody interpretations and inserted well tops in the seismic section window along cross-sections PP' and RR' (a) the gas cap in reservoir R2(B) is identified on the seismic time slice of the envelope attribute cube; (b) the geobody-based contact surfaces show remarkable conformity to the reservoir inclination; (c) Extending the map beyond the reservoir edges to the boundary of a closed polygon, results in warped surfaces of the geobody-based maps, causing a discrepancy in contact angle; (d) in comparison, the map built using the inserted horizon tops has a smoother surface.

a result, the derived maps exhibited improved alignment with the dipping plane of hydrocarbon contacts (Fig. 13a). Extending the geobody interpretations further enhanced the alignment with the inclinations of hydrocarbon contacts across significant portions of the field, facilitating the tracking of oil-water contacts across multiple wells. Nonetheless, a notable limitation is the susceptibility to seismic data noise, leading to misalignment with contact depths in certain wells and deviations observed in the seismic section window. Figure 13b highlights the misalignment at gas contact depths in Well- C1, as also evident in the oval shapes on the seismic section window (Fig. 13c). This discrepancy may stem from the stretching of contact maps during the smoothening process, extraction of geobodies affected by structural uplift, or extraction of irrelevant geobodies proximal to those of interest. While these discrepancies may be disregarded if occurring distant from reservoir locations, their effects were addressed through horizon interpretation edits. Furthermore, in specific instances, these errors can be rectified through partitioning the contact map using closed polygons for individual reservoirs and adjusting their depth values to align with hydrocarbon contacts at each reservoir location.

It is essential to exercise caution when employing the horizon-based method for generating contact maps, particularly in instances where a fault exists between

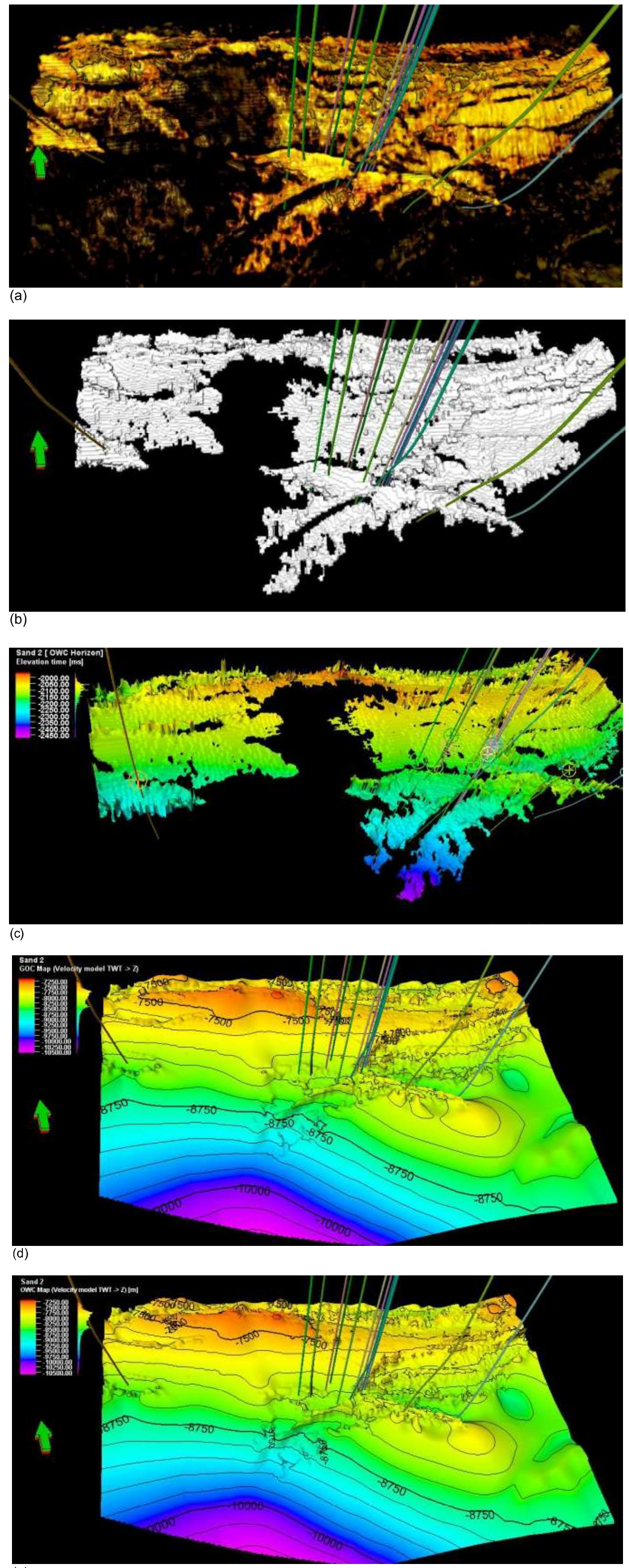

Figure 12: The workflow in generating geobody-based contact maps starts with (a) highlighting the reservoir geobodies (b) extracting the geobodies; (c) converting the extracted geobodies into horizons and to (d) gas-oil contact map and (e) oil-water contact map.

adjacent wells. This is attributed to the heightened probability of misaligning the horizon-based contact maps with the hydrocarbon contacts due to the close proximity of wells on opposing sides of a fault line. This discrepancy often becomes evident upon the application of smoothing to a map, resulting in the transformation of sharp edges to smoother contours as curves are utilized to interconnect segments of the map spanning both sides of the fault throw. Furthermore, if a substantial vertical distance exists between the hanging wall and the footwall, the maps may be elongated below the actual point of fluid contact in any well drilled in close proximity to the fault edge. This observable phenomenon is denoted by a yellow circle on the horizon-based maps (Fig. 13d).

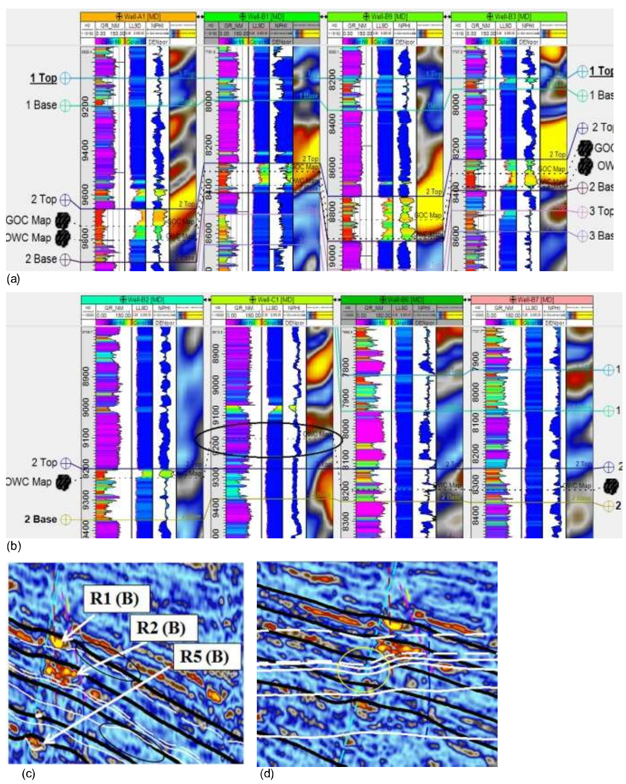

Figure 13: Well correlation using contact maps; (a) the extensive geobody-based contact maps accurately identified the gas-oil/oil-water contacts in the reservoirs across the field; (b) the error in extracting geobodies can give rise to misaligned contact maps in some wells; (c) the error is usually due to extraction of geobodies in close proximity (oval shapes); and (d) the inclusion of wells across a fault throw when generating contacts with inserted horizon tops can give rise to inaccurate maps.

On the other hand, excluding these wells from the interpretation can remove or reduce the error but also reduces the available wells, resulting to low density of horizon points used in building the contact maps. These shortfalls can be avoided by employing geobody-based interpretations when creating those maps. In addition, the envelope attribute identified other locations in Sand 2 where they are hydrocarbon reservoirs the northeastern part of the field (R2(D))

The results discussed thus far, show that the application of the envelope attribute is an interactive process which ensures more accurate results. Figure 14 below contrasts the results of the two procedures used in building hydrocarbon contact maps.

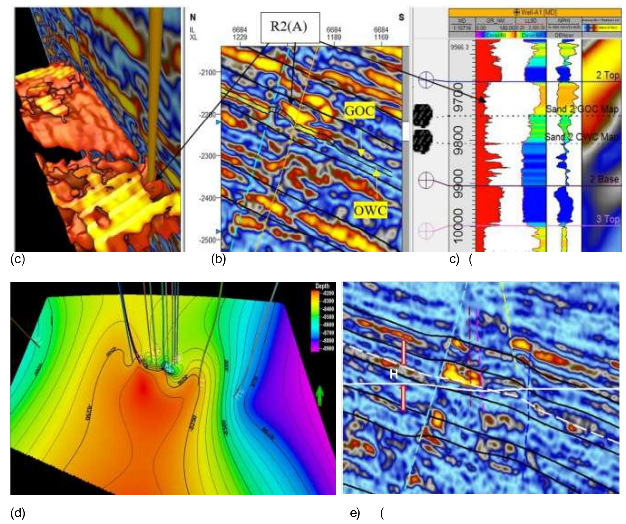

Figure 14: The advantage of creating contact maps using the geobody-based horizons is that it can be quality-controlled in real time; (a)-(c) extraction of geobodies and maps built with it can be viewed simultaneously; (d) contact maps generated using a single value for contact depth or inserted well tops can be unrealistic, and can cause erroneous estimates; (e) wrong angle of fluid contact, H, can cause huge discrepancies in reserve estimates. The slanting, dashed, white line is the geobody-based oil-water contact map, the continuous white, horizontal line is the oil-water contact maps built using inserted horizon tops, the black slanting lines are the top horizons and the vertical dashed lines are fault lines.

The HIIP (hydrocarbon initially in place) maps for reservoir 2 are depicted in Figures 15(a) and 15(b), showcasing the contact maps created using inserted horizon tops and body-based contact maps, respectively. The influence of the different hydrocarbon contact maps is evident in the HIIP maps, subsequently impacting the HIIP estimates. Discrepancies in the volume estimation of the reservoir are attributed to variances in the reservoir boundaries, particularly in zones A and B. In addition, the reservoir in zone A has more gas than that in zone B which is as a result of accumulated gaseous hydrocarbons migrating from lower reservoirs as seen earlier in Figure 7.

The former (Fig 16a) exhibits broader contours and edges, resulting in a larger area and higher HIIP estimates, while

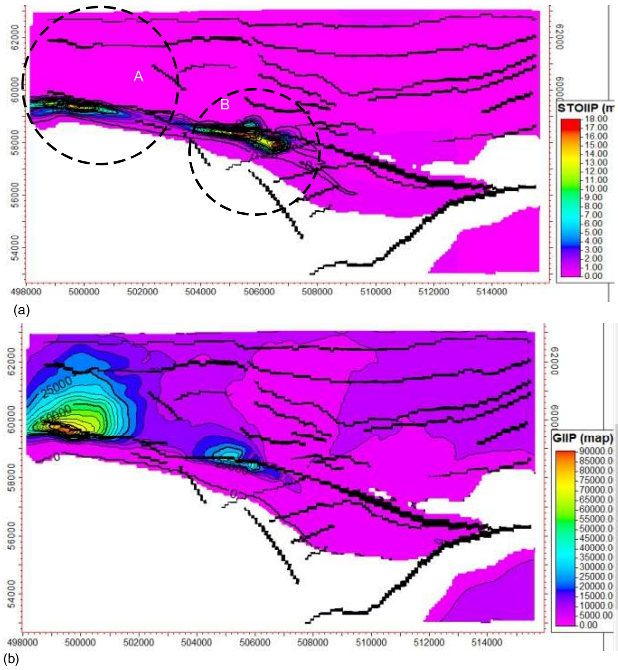

Figure 15: The HIIP volume maps for reservoir 2 utilizing contact maps built using inserted horizon tops yielded smoother closures for (a) stock tank oil initially in place and (b) gas initially in place.

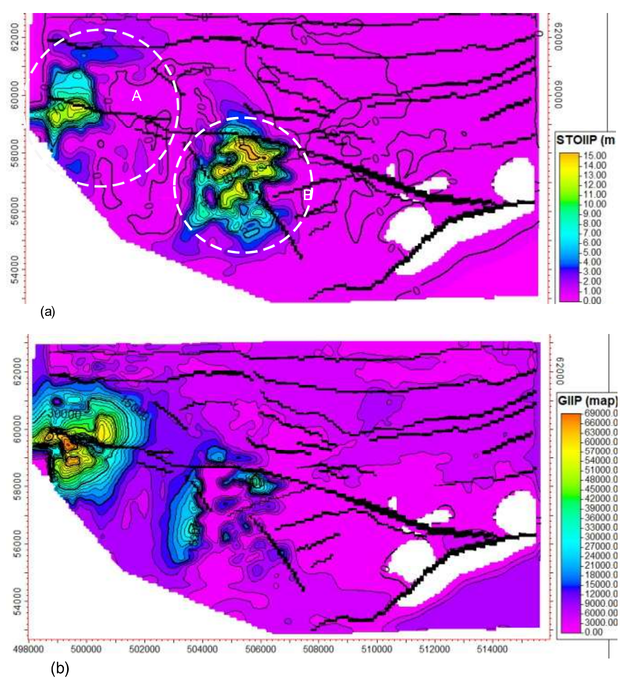

Figure 16: The GIIP and STOIIP volume maps for reservoir 2 obtained utilizing contact maps built using extracted seismic geobodies yielded closures in conformity with the fault lines for both (a) stock tank oil initially in place and (b) gas initially in place.

the latter (Fig. 16b) demonstrates enhanced consistency with the fault interpretations in zones A and B of the field, leading to lower volume estimates. For instance, the GIIP estimate for reservoir 2 obtained using the contact maps from the extracted geobodies yielded a value of 11099910 MMSCF of gas, whereas the former provided a value of 8425696 MMSCF of gas, reflecting a significant increase. This variation can be attributed to the differing positions of the contact maps indicated as 'H', as expounded upon in the preceding paragraphs. Also, the zone D part of the field can be explored for possible accumulations of substantial volumes of hydrocarbons.

Table 1: Comparison of the estimated hydrocarbon volumes from the reservoirs using the contact surfaces obtained from both methods.

HIIP (from geobody based contact maps)			HIIP (from horizon-based contact maps)	
RES.	STOIIP (MMsm³)	GIIP (MMSCF)	STOIIP (MM sm³)	GIIP (MMSCF)
2	112	11099910	20.3	8425696

Summary

This study has showcased the utilization of envelope attributes for the generation of reservoir hydrocarbon contact maps, presenting a swifter and more precise method compared to existing approaches. The findings have underscored the strong correlation between the obtained surface maps and well-log stratigraphic markers, facilitating the identification of reservoir contacts and alignment with reservoir topography, thereby enhancing the accuracy of hydrocarbon volume estimates. Moreover, the contact maps can be adjusted to better align with hydrocarbon contacts in certain scenarios. The envelope attribute has also identified unexplored regions in the R2(D) field for potential hydrocarbon exploration and has detected the presence of gas along fault planes, thus offering valuable insights for fault seal analysis. Notwithstanding these advantages, a prominent drawback of this method is its suboptimal performance with oil reservoirs, as they often lack the high impedance contrast required by the envelope attribute. Additionally, the envelope attribute is susceptible to data quality issues and may inadvertently incorporate outliers within its range, necessitating potential editing to mitigate map roughness. Nevertheless, given the substantial benefits outweighing the limitations, it is recommended to adopt this workflow for enhanced reservoir evaluation.

Funding: this research did not receive any specific grant from funding agencies in the public, commercial, or not-for-profit sectors.

REFERENCES CITED

Alsouki, M., Taifour, R., Al Hamad, O., (2014). Delineating the Fluvial Channel System in the Upper Triassic Formation of the Elward area in the Syrian Euphrates Graben Using 3-D seismic attributes. Journal of Petroleum Exploration and Production Technology. 4, 123–132. https://doi.org/10.1007/s13202-014-0110-5

Avbobo, A. A., (1978). Tertiary Lithostratigraphy of Niger Delta. American Association of petroleum geologists Bulletin, 62, 295-300.

Ayolabi, E.A, Adigun, A.O., (2013). The Use of Seismic Attributes to Enhance Structural Interpretation of Z-Field, Onshore Niger Delta. Earth Science Research. 2(2), 223-238.

Corredor, F., Shaw J.H, Bilotti F., (2005). Structural Styles in the Deepwater Fold And Thrust Belts of the Niger Delta. AAPG Bull 89(6), 753–780

Dennis ,H., Bergmo ,P., Holt, T, (2005).Tilted Oil–Water Contacts: Modelling the Effects Of Aquifer Heterogeneity. In: DORE ,A.G.&VINING ,B.A.(eds) Petroleum Geology: North-West Europe and Global Perspectives—Proceedings of the 6thPetroleum Geology Conference, Petroleum Geology Conferences Ltd. Published by the Geological Society, London, 145–158.

Doust H. and Omatsola M., (1990). Divergent and Passive Margin Basins. American Association of Petroleum Geologist Bulletin, 48(1), 201-238.

Dolson J., (2016). Understanding Seals, Pressures, and Hydrodynamics. In Understanding Oil and Gas Shows and Seals in the Search for Hydrocarbons, Springer, Cham, 145-232

Ejedawe, J. E., 1981. Patterns of incidence of oil reserves in Niger Delta Basin. American Association of Petroleum Geologists (AAPG), 65.

Evamy, B.O., Herembourne, J., Kameline, P., Knap, W.A., Molloy, F.A., Rowlands, P.H., (1978). Hydrocarbon habitat of Tertiary Niger Delta. American Association of Petroleum Geologists Bulletin. 62,1-39.

Ismail, A., Zollo, A., (2020). Identification of Gas Zones and Chimneys Using Seismic Attributes Analysis at the Scarab Field Offshore Nile Delta, Egypt. Petroleum Research. 5(1), 59-69.

Megson, J.B., (1992). The North Sea Chalk Play: Examples from the Danish Central Graben. In :Hardman, R. F. P. (ed.) Exploration Britain: Geological Insights for the Next Decade. Geological Society, London, Special Publications, 67,247–282.

Nanda, N.C., (2016). Analysing Seismic Attributes. In: Seismic Data Interpretation and Evaluation for Hydrocarbon Exploration and Production 10.1007/978-3-319-26491-2.

Ouadfeul, S.A., Aliouane, L., (2014). Fractal Analysis of AVO Seismic Attributes for Oil/Water Contact Identification. 10.1007/978-3-642-32408-6_136.

Sarhan, M.A., (2017). The Efficiency of Seismic Attributes to Differentiate Between Massive and Non-Massive Carbonate Successions for Hydrocarbon Exploration Activity. NRIAG Journal of Astronomy and Geophysics. Retrieved from: http://dx.doi.org/10.1016/j.nrjag.2017 on 10th July, 2020.

Short, K.C., Stauble, A.J., (1967). Outline of the Geology of the Niger Delta. American Association of Petroleum Geologist Bulletin. 51, 761-779.

Subrahmanyam, D., Rao P.H., (2008). Seventh International Conference and Exposition on Petroleum Geophysics, Seismic Attributes a Review. 398.

Taner, M.T., Sheriff, R.E., (1977). Application of Amplitude, Frequency and other Attributes to Stratigraphic and Hydrocarbon Determination. AAPG Memoir. 26, 301-328.

Taner, M.T., Koehler, F, Sheriff, R.E., (1979). Complex Seismic Trace Analysis, Geophysics. 44,1041–1063.

Yan P., Kalscheuer T., Hedin P., Garcia J.M.A., (2017). Two Dimensional Magnetotelluric Inversion Using Reflection Seismic Data as Constraints and Application in the COSC Project, Geophysics. Res. Lett. 44,3554–3563.

Wang, C., Shi, Z., Sun, Y., Wang, X., Zhou, H., (2015). Quantitative Analysis Method of Seismic Attributes Under Limited Well Control Conditions and Its Application to Source Rock Prediction. Arabian Journal of Geosciences. 3417-3425. https://doi.org/10.1007/s12517-014-1445-4

Weber, K.J., Daukoru, E.M., (1975). Petroleum geology of the Niger Delta. Proceedings of the 9th World Petroleum Congress, Tokyo. 2, 202- 221.

Whiteman, A.J., (1982). Nigeria, Its Petroleum Geology, Resources and Potential. Graham and Trottan, London. 1&2, 394.